Progress in PHOTOVOLTAICS

PROGRESS IN PHOTOVOLTAICS: RESEARCH AND APPLICATIONS
Prog. Photovolt: Res. Appl. 2014; **22**:515–524
Published online 29 October 2012 in Wiley Online Library (wileyonlinelibrary.com). DOI: 10.1002/pip.2285

RESEARCH ARTICLE

Analysis of temperature coefficients for III–V multi-junction concentrator cells

Gerald Siefer* and Andreas W. Bett

Fraunhofer Institute for Solar Energy Systems ISE, Heidenhofstr. 2, 79110 Freiburg, Germany

ABSTRACT

The temperature dependence of the *I–V* parameters of different III–V multi-junction concentrator cells at several concentration levels was investigated. Moreover, the influence of spectral changes on the temperature coefficients of multi-junction solar cells was examined. Complete sets of temperature coefficients of a metamorphic $Ga_{0.35}In_{0.65}P/Ga_{0.83}In_{0.17}As$ dual-junction cell, a metamorphic $Ga_{0.35}In_{0.65}P/Ga_{0.83}In_{0.17}As/Ge$ triple-junction cell and a lattice-matched $Ga_{0.50}In_{0.50}P/Ga_{0.99}In_{0.01}As/Ge$ triple-junction cell determined under well-controlled laboratory conditions are reported. Copyright © 2012 John Wiley & Sons, Ltd.

KEYWORDS

mult-junction cells; concentrators; temperature dependence

***Correspondence**

Gerald Siefer, Fraunhofer Institute for Solar Energy Systems ISE, Heidenhofstr. 2, 79110 Freiburg, Germany.
E-mail: gerald.siefer@ise.fraunhofer.de

Received 25 February 2012; Revised 18 July 2012; Accepted 3 August 2012

1. INTRODUCTION

Megawatt-level concentrator systems applying III–V multi-junction cells have recently been installed [1]. This accomplishment clearly demonstrates the growing interest in concentrator technology. Predicting the energies of concentrating photovoltaic systems using triple-junction solar cells remains a challenge [2–6]. The outputs of such systems are strongly influenced by the environment, such as circumsolar radiation, the seasonal and daily changes in the solar spectrum, effects resulting from the concentrating optics, including chromatic aberrations for lenses or reflectivity for mirrors, wind speed and operating cell temperature. The operating cell temperature itself is influenced by the environment (ambient temperature, irradiance and wind speed) and the mounting process technology (thermal resistance). Thus, knowledge of the temperature dependence of the *I–V* parameters of solar cells is essential for predicting the performance of photovoltaic systems. In particular, the temperature coefficient of a concentrator solar cell depends on the applied concentration level [7]. The temperature coefficient decreases with increasing illumination intensity, and the very low value of −0.1%/K has been already reported for the open circuit voltage temperature coefficient of a GaAs solar cell at 1000× concentration [8]. Detailed analyses of III–V multi-junction concentrator solar cells remain scarce [9–19]. Moreover, the performance of a III–V multi-junction solar cell is sensitive to spectral changes [20–23], and the temperature coefficients of multi-junction solar cells may also be dependent on spectral changes. However, this subject has to be investigated. In this paper, we applied the spectrometric characterisation technique to analyse the spectral dependence of the temperature coefficients. We also report the temperature coefficients of the voltage and the maximum power of a lattice-matched $Ga_{0.50}In_{0.50}P/Ga_{0.99}In_{0.01}As/Ge$ triple-junction cell and metamorphic $Ga_{0.35}In_{0.65}P/Ga_{0.83}In_{0.17}As$ dual-junction and $Ga_{0.35}In_{0.65}P/Ga_{0.83}In_{0.17}As/Ge$ triple-junction cells. These cells were investigated over a wide range of concentrations under well-controlled laboratory conditions. In the following, a theoretical treatment of the principal correlations among voltage, temperature and concentration is presented. Subsequently, a routine for temperature-dependent calibration of multi-junction solar cells, including temperature-dependent spectral response measurements, 1-sun *I–V* curve, spectrometric characterisation and finally the temperature-dependent calibration under concentration, is described.

2. THEORY

We use the single-diode model to describe the solar cell's *I–V* characteristics and derive the temperature dependence of the open circuit voltage V_{OC}:

$$J(V) = J_0\left(e^{\frac{qV}{nkT}} - 1\right) - J_{photo} \quad (1)$$

where J_0 is the diode's dark saturation current, q is the electric charge, n is the ideality factor, k is Boltzmann's constant, T is temperature and J_{photo} is the photo current of the cell.

Setting $J(V_{OC})=0$ produces the well-known expression for V_{OC}:

$$V_{OC}(T,C) = \frac{nkT}{q}\ln\left(\frac{J_{photo}}{J_0(T)}+1\right) \cong \frac{nkT}{q}\ln\left(\frac{J_{SC}}{J_0(T)}\right) = \frac{nkT}{q}\ln\left(\frac{C * J_{SC,1\ sun}}{J_0(T)}\right) \quad (2)$$

where $J_{SC,1\ sun}$ is the short circuit current of the cell at standard testing conditions equivalent to 1 sun and C is the concentration ratio assuming a linear behaviour between J_{SC} and concentration level.

In the following section, we analyse two limiting cases: (i) the diode quality factor equals 1, and the dark saturation current is thus dominated by bulk and surface recombination; and (ii) the diode quality factor equals 2, and the dark saturation current is thus dominated by recombination within the space charge region and/or the perimeter.

2.1. The saturation current is dominated by bulk recombination

In this case, J_0 and n are replaced by J_{01} and n_1, where n_1 is close to unity and J_{01} is given by the following [24]:

$$J_{01}(T) = q * n_i^2(T) * \left(\frac{D_e(T)}{N_A * L_e(T)} + \frac{D_h(T)}{N_D * L_h(T)}\right) \quad (3)$$

where n_i is the intrinsic carrier concentration, D_e (D_h) is the diffusion coefficient of the electrons (holes) in the p-doped base (n-doped emitter), N_A (N_D) is the majority carrier density in the base (emitter) and L_e (L_h) is the diffusion length of the electrons (holes) in the base (emitter). For typical emitter and base doping levels of N_D ~$10^{18}\,cm^{-3}$ and N_A ~$10^{17}\,cm^{-3}$, the second term in the parentheses can be neglected.

Using the following equation for the diffusion length:

$$L_e = \sqrt{D_e\tau_e} \quad (4)$$

with τ_e representing the carrier lifetime of the electrons in the base leads to the following expression for J_{01}:

$$J_{01} \cong q\left(\frac{D_e}{\tau_e}\right)^{1/2}\frac{n_i^2}{N_A} \quad (5)$$

The following equation determines the intrinsic carrier density n_i in terms of the band gap energy E_g [24]:

$$n_i^2 \propto T^3\exp\left(\frac{-E_g(T)}{kT}\right) \quad (6)$$

Neglecting any temperature dependence of D_e/τ_e in the temperature range of interest for terrestrial photovoltaic applications [7,25,26], equation 5 can be expressed as

$$J_{01}(T) = B_1T^3\exp\left(\frac{-E_g(T)}{kT}\right) \quad (7)$$

where B_1 is a constant independent of temperature.

The temperature dependence of the bandgap is typically expressed using the Varshni relation [27,28]:

$$E_g(T) = E_g(0) - \frac{\alpha T^2}{T+\beta} \quad (8)$$

where α and β are material-dependent constants and $E_g(0)$ corresponds to the band gap energy at 0 K.

After substituting for J_0 in equation 2, using equations 7 and 8 and introducing the thermal voltage V_T and the band gap voltage V_g,

$$V_T = \frac{kT}{q} \quad V_g = \frac{E_g}{q} \quad (9)$$

equation 2 can be differentiated with respect to temperature, yielding the temperature coefficient $TC(V_{OC})$ of the open circuit voltage:

$$\frac{dV_{OC}}{dT} = \frac{d}{dT}\left(\frac{kT}{q}\ln\left(\frac{J_{SC}}{J_{01}}\right)\right) = -\frac{(V_g - V_{OC}) + 3V_T}{T} + V_T\left(\frac{1}{J_{SC}}\frac{d}{dT}J_{SC} + \frac{1}{V_T}\frac{d}{dT}V_g\right) \quad (10)$$

Equation 10 leads to negative values, as the modulus of the first term is larger than the modulus of the second term; that is, the open circuit voltage decreases with increasing temperature. A solar cell with a larger V_{OC} exhibits lower sensitivity to temperature changes, as $(V_g - V_{OC})$ will decrease in this case.

2.2. The saturation current is dominated by recombination in the depletion zone

At low irradiance levels, the dark saturation current of solar cells is often dominated by recombination in the depletion zone. In this case, J_0 and n are replaced by J_{02} and n_2, respectively, where n_2 is approximately 2 and J_{02} is given by the following [24]:

$$J_{02} = \frac{n_i W_d kT}{2(V_d - V)\tau_{n0}} \quad (11)$$

where W_d is the width of the depletion zone, V_d is the diffusion voltage and τ_{n0} is the minimum electron lifetime. Assuming that the main temperature dependence of J_{02} arises from n_i, the following expression for J_{02} is obtained:

$$J_{02} = B_2Tn_i = B_2T^{2.5}\exp\left(\frac{-E_g(T)}{2kT}\right) \quad (12)$$

where B_2 again is a constant independent of temperature. Using the Varshni relation for $E_g(T)$ (equation 8) and substituting the thermal and band gap voltages (equation 9) lead to the following:

DOI: 10.1002/pip

$$\frac{dV_{OC}}{dT} = \frac{d}{dT}\left(\frac{n_2 kT}{q}\ln\left(\frac{J_{SC}}{J_{02}}\right)\right) = -\left(\frac{\left(\frac{n_2}{2}V_g - V_{OC}\right) + n_2 2.5V_T}{T}\right) + n_2 V_T\left(\frac{1}{J_{SC}}\frac{d}{dT}J_{SC} + \frac{1}{V_T}\frac{d}{dT}V_g\right) \quad (13)$$

As in the case of equation 10, the result of equation 13 is negative, as the modulus of the first term is larger than the modulus of the second term; that is, the open circuit voltage again decreases with increasing temperature. Equation 13 also demonstrates the positive influence of a high V_{OC}, represented by the term $[(n_2/2)V_g - V_{OC}]$.

In both cases, the following relation between the open circuit voltage and the concentration is valid:

$$V_{OC}(T,C) = \frac{n_{1/2}kT}{q}\ln\left(\frac{J_{SC}}{J_{01/02}}\right) = V_{OC}(T,1x) + \frac{n_{1/2}kT}{q}\ln(C) \quad (14)$$

Thus, V_{OC} increases with concentration, and the temperature coefficient of the open circuit voltage therefore decreases with concentration:

$$\frac{dV_{OC}}{dT}|_{T,C} = \frac{d}{dT}\left(V_{OC}(T,1x) + \frac{n_{1/2}kT}{q}\ln(C)\right) = \frac{dV_{OC}}{dT}|_{T,1x} + \frac{n_{1/2}k}{q}\ln(C) \quad (15)$$

In summary, this result means that a high V_{OC} is desirable because it makes the open circuit voltage less sensitive to temperature changes. This high V_{OC} can be obtained by a low dark saturation current and/or operation under concentrated light.

To analyse the temperature coefficient of the open circuit voltage in more detail, the magnitudes of each term contributing to equations 10 and 15 are plotted in Figure 1. The calculations were performed for a GaAs solar cell. Other semiconductor materials will obey the same trends but exhibit different absolute values. The left portion of Figure 1 corresponds to an illumination level of 1 sun, that is, 1000 W/m^2. Equation 13 was used for the calculation, as the behaviour of concentrator cells at low intensities is dominated by recombination processes described by the dark saturation current J_{02}. The right portion of Figure 1 shows the results corresponding to an illumination level of 1000×. Here, equations 15 and 10 were used to derive the data because the solar cell characteristics at high concentrations are best described using the dark saturation current J_{01}. The following input parameters were used in these calculations. The Varshni parameters for GaAs were chosen according to reference [28]: $\alpha = 5.405$, $\beta = 204$ K and $E_g(0) = 1.519$ eV. The J_{SC} at 1 sun of illumination and the relative temperature coefficient dJ_{SC}/dT were set to the means of the measured values for GaAs concentrator cells (27.5 mA/cm^2 and 0.075%/K [8]). The parameters B_2 in equation 12 and B_1 in equation 7 were set to 6.5×10^{-5} and 0.02, respectively, to match the dark saturation currents J_{02} and J_{01} of the measured GaAs concentrator cells and therefore to match V_{OC} at concentrations of 1× and 1000× [8].

Figure 1 clearly demonstrates the positive effect of a high open circuit voltage on the temperature dependence of V_{OC}. Comparing the temperature coefficient of V_{OC} operating at 1 (Figure 1 left) and 1000 suns of illumination (Figure 1 right), the primary reduction in the temperature dependence is caused by the term $-(V_g - V_{OC})/T$; therefore, a high open circuit voltage is expected to reduce the temperature-related losses in V_{OC}. Note that dV_{OC}/dT also depends slightly on temperature itself, which is mainly due to the term $-(V_g - V_{OC})$. Figure 2 compares the calculated values of V_{OC} at $T = 25$ °C and the temperature coefficient of V_{OC} with values measured using five GaAs concentrator cells. The areas of the GaAs concentrator cells varied from 0.01 to 0.13 cm^2. The theoretical values were determined separately for the cases in which the solar cell behaviour was dominated by recombination described by J_{02}/n_2 or J_{01}/n_1.

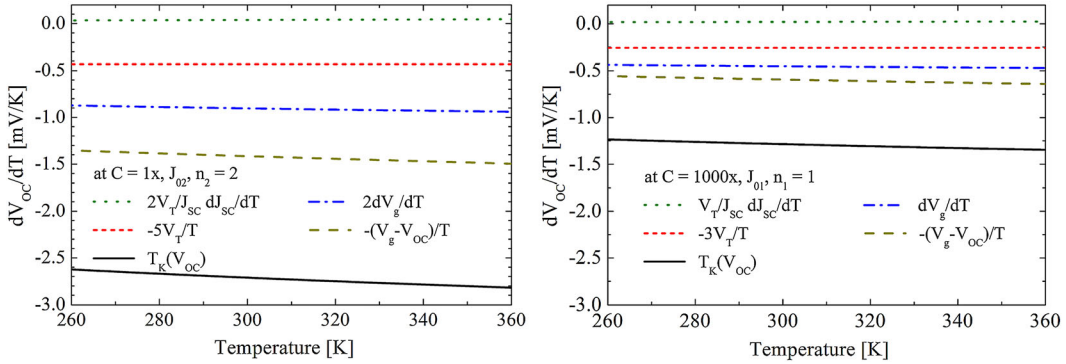

Figure 1. Contributions to the temperature coefficient of the open circuit voltage V_{OC} of a GaAs cell. Left: Operation at 1-sun illumination, that is, 1000 W/m^2. Equation 13 (J_{02}, n_2) was used to describe the solar cell's behaviour. Right: Equation 15 in combination with equation 10 (J_{01}, n_1) was used to describe the solar cell's behaviour at 1000×. The input parameters are given in the text. dV_{OC}/dT depends slightly on the temperature primarily because of the term $-(V_g - V_{OC})/T$.

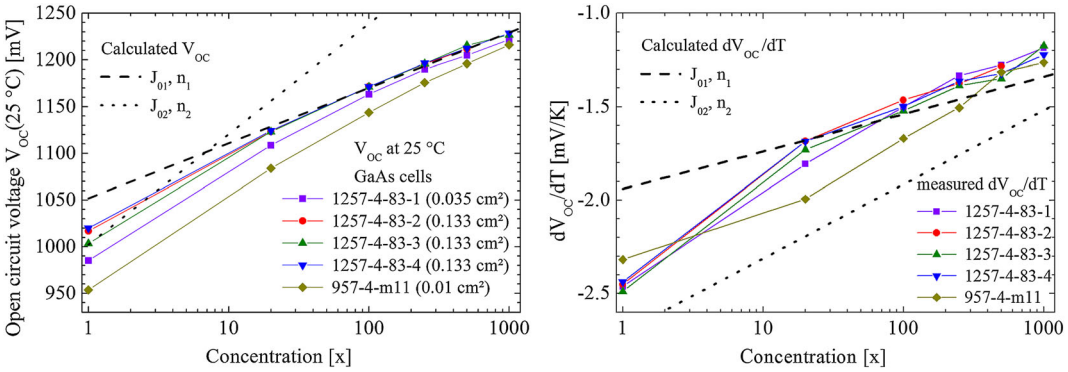

Figure 2. Comparison of experimental and calculated V_{OC} values (left) and the temperature coefficient dV_{OC}/dT (right) for five GaAs concentrator cells versus concentration. The calculated values were determined assuming that the *I–V* characteristics of the solar cell were dominated by J_{02}/n_2 or J_{01}/n_1 and plotted together with the measurement results.

V_{OC} in Figure 2 exhibits deviations from a logarithmic increase versus concentration, which corresponds to a non-linear behaviour in the semi-logarithmic scaling of the *x*-axis. In this context, it is important to mention that the flattening of the curve for higher concentrations cannot be explained by a possible heating of the cell during the *I–V* curve measurement. The temperature-dependent measurements under concentration were performed using the FlashSim flash simulator of the ISE CalLab [8]. Every *I–V* curve measurement presented in this paper actually corresponds to the average of two single *I–V* curve measurements performed during two successive flashes. During the first *I–V* curve, the voltage is switched from zero (i.e. I_{SC}) to V_{OC}, whereas during the next flash, the *I–V* curve is recorded switching voltage from V_{OC} to I_{SC}. As the differences found for V_{OC} between the two voltage sweeping directions for all cells and concentrations was always well below 0.1%, a heating of the cell during *I–V* curve measurement can be excluded for the concentration range investigated here. Thus, the graphs in Figure 2 demonstrate that the measured values of V_{OC} and the temperature coefficient cannot be described by the single-diode model solely. At low concentrations, the measured open circuit voltage (Figure 2, left) and the temperature coefficient of V_{OC} (Figure 2, right) both exhibit greater increases with concentration compared with operation under high irradiances. A comparison of the measured and calculated values of V_{OC} (Figure 2, left) suggests that the behaviour of solar cells is better described using J_{02}/n_2 at low concentrations. However, at high concentrations, the relationship between V_{OC} and concentration can only be described by J_{01}/n_1. The predicted temperature coefficient of V_{OC} follows the same trend as the predicted V_{OC}. Again, the relationship between dV_{OC}/dT and concentration suggests that J_{02}/n_2 dominates the solar cell behaviour at low concentrations and J_{01}/n_1 becomes important at high concentrations. The solar cell area of the GaAs cells from Figure 2 varies between 0.01 and 0.133 cm^2 — the actual values are given in the legend of Figure 2 (left). It is known that for smaller cell areas, an increase in dark saturation current J_{02} can be found because of the higher influence of the cell's perimeter [29–31]. This can explain the lower V_{OC} of cells 1257-4-83-1 and 957-4-m11 compared with cells 1257-4-83-2, -3 and -4 with higher cell area. Additionally, the difference found in V_{OC} between cells 1257-4-83-1 and 957-4-m11 with small area and cells 1257-4-83-2, -3 and -4 becomes smaller for higher concentration ratios where the cell behaviour is better described by J_{01}/n_1. However, the absolute values of dV_{OC}/dT are not fully reproduced, indicating that some of the simplifications made from equations 3 to 7 and from equations 11 to 12 are not fully valid.

3. MEASUREMENT PROCEDURE TO DETERMINE THE TEMPERATURE COEFFICIENT

Our procedure to determine the temperature coefficients of the solar cells involves three steps:

i. Temperature-dependent spectral response measurements are taken, enabling the spectral mismatch correction [23,32] using the spectral response determined at the corresponding temperature.
ii. Temperature-dependent *I–V* curves under 1 sun of illumination (AM1.5d, 1000 W/m^2) are then recorded as a function of solar cell temperature.
iii. *I–V* curves as functions of concentration are recorded at different temperatures.

3.1. Spectral response

The temperature-dependent spectral response measurements were performed on all cells presented in this paper. As an example, Figure 3 shows the external quantum efficiency (EQE) of a lattice-matched $Ga_{0.50}In_{0.50}P/Ga_{0.99}In_{0.01}As/Ge$ triple-junction cell (1797-6-129-8, cell area: 4 cm^2) at 10 and 70 °C.

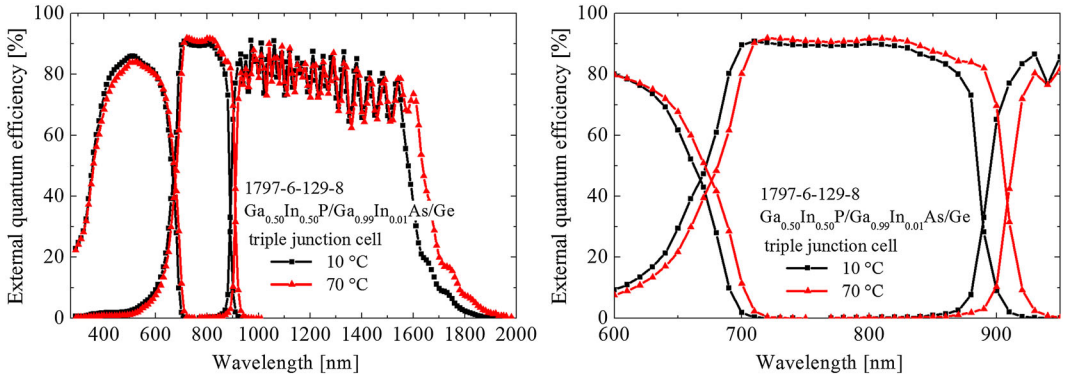

Figure 3. Measured external quantum efficiency of the lattice-matched $Ga_{0.50}In_{0.50}P/Ga_{0.99}In_{0.01}As$/Ge triple-junction cell 1797-6-129-8 at 10 and 70 °C. The left plot shows the complete wavelength range, whereas the right plot only shows the wavelength region of the middle subcell.

Because the band gaps of the semiconductor materials involved decrease with increasing temperature (compare also equation 8), the response region of the subcells expands towards higher wavelengths in Figure 3. However, the EQE also decreases at low wavelengths as a result of the additional absorption in the subcell above (see Figure 3, right). This finding directly implies that the current of the whole multi-junction cell will not always increase with temperature; see also [10,33].

3.2. *I–V* characteristics at 1 sun and spectrometric characterisation

Because the subcells are connected in series, multi-junction cells are more sensitive than single-junction devices to changes in the incident spectrum. Therefore, the temperature dependence of multi-junction solar cell parameters can be expected to depend on the incident spectrum. To clarify this issue, spectrometric characterisations were performed at different temperatures. Spectrometric characterisation is a tool for quantifying the effect of changes in the incident spectrum on the performance of multi-junction cells [23]. This technique involves systematically changing the spectrum of the sun simulator. As an example, Figure 4 shows the temperature-dependent spectrometric characterisation of the metamorphic $Ga_{0.35}In_{0.65}P/Ga_{0.83}In_{0.17}As$ dual-junction cell 840-5-9.

Figure 4 shows the typical characteristics derived by spectrometric characterisation and the influence of temperature on these characteristics. The short circuit current density J_{SC} increases with temperature. The maximum value of J_{SC}, approximately at 1.00, corresponds to current-matching conditions. Interestingly, the position of the maximum J_{SC} on the x-axis does not shift with temperature. Therefore, for the investigated dual-junction cell 840-5-9, the absolute gains in current with increasing temperature are almost equal for the top and bottom subcells, although the bottom subcell experiences a decrease in spectral response at lower wavelengths as a result of the extended response of the top cell. For example, compare the EQE of the middle subcell in Figure 3. The same behaviour was observed in the triple-junction solar cells.

The fill factor (*FF*) trends oppositely to the short circuit current density, decreasing with increasing temperature. At a fixed temperature, the minimum *FF* corresponds to current-matching conditions, as this case does not involve shifts in the subcells' operating voltages because of current differences [23,34].

The open circuit voltage V_{OC} exhibits a strong decrease with increasing temperature (compare equations 10 and 13); however, the V_{OC} at a fixed temperature is almost independent of the position on the x-axis. This observation reflects that changing the incident spectrum decreases the current of one subcell but increases the current of the other. To the first order, the resulting small changes in the V_{OC} values of the two subcells cancel each other out.

The maximum power point P_{Mpp} behaves opposite to the short circuit current density J_{SC}; that is, it decreases as the temperature increases. When moving away from current-matching conditions at a fixed temperature, the losses in current are partly compensated for by the gain in fill factor. Therefore, the maximum power P_{Mpp} is less affected by changes in the spectrum than J_{SC}.

The temperature coefficients for all of the *I–V* parameters in Figure 4 (left) were determined by linear regression. Note that only three data points were available to determine the temperature coefficients at $x = 0.94$ on the lower x-axis, which explains the deviation of $TC(V_{OC})$ at $x = 0.94$. The temperature coefficients of the maximum power point P_{Mpp}, the short circuit current density J_{SC} and the open circuit voltage V_{OC} do not exhibit strong dependence on the incident spectrum (i.e. they do not depend strongly on the position on the x-axis). The fill factor seems to have a slightly weaker temperature dependence when the current is limited by the bottom cell (x values > 1.04 on the bottom x-axis) — −0.75 versus −0.6%/K — however, the differences are still small (Figure 4, right).

In summary, the spectrometric characterisation of the metamorphic $Ga_{0.35}In_{0.65}P/Ga_{0.83}In_{0.17}As$ dual-junction cell 840-5-9 (Figure 4) resolves the influences of the incident

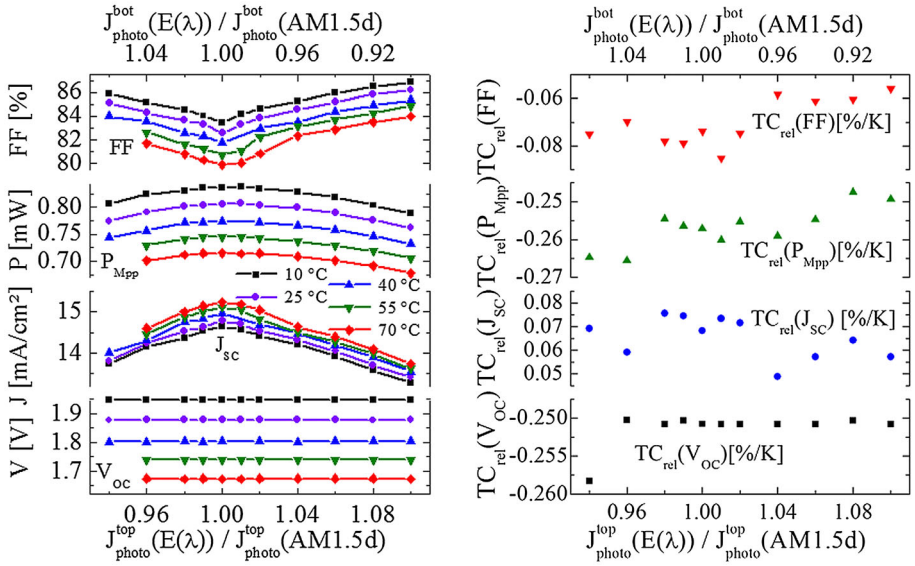

Figure 4. Left: Temperature-dependent spectrometric characterisation of the Fraunhofer ISE $Ga_{0.35}In_{0.65}P/Ga_{0.83}In_{0.17}As$ dual-junction cell 840-5-9. The point 1.00 on the *x*-axis corresponds to the spectra that generate the same current in the top and bottom subcells as AM1.5d. Right: Spectral-dependent relative temperature coefficients determined by applying linear regression to the temperature-dependent *I–V* parameters shown in the left graph.

spectrum and temperature on the solar cell parameters. However, the temperature dependences of the solar cell parameters are not significantly sensitive to the incident spectrum.

3.3. Temperature-dependent measurements under concentration

As in the case of the GaAs cells shown before (compare Figure 2), the temperature-dependent measurements under concentration were performed using the FlashSim flash simulator of the ISE CalLab [8]. As an example, Figure 5 shows the measured *I–V* parameters, the open circuit voltage V_{OC}, the fill factor *FF* and the efficiency η of the $Ga_{0.50}In_{0.50}P/Ga_{0.99}In_{0.01}As/Ge$ concentrator cell 1797-4-129-SCA-44 versus concentration and at different temperatures. The concentration in Figure 5 was determined using the cell's short circuit current under 1 sun of illumination at the corresponding temperature.

The data shown in Figure 5 reveal that the temperature dependence of the presented *I–V* parameters decreases as the concentration ratio increases. As in the case of the GaAs cells shown previously (see Figure 2), a stronger increase in V_{OC} for low concentration ratios is observed, suggesting again a domination of the cell behaviour by J_{02}/n_2 at low concentration ratios. Note again that heating of the cell during the measurement can be excluded as reason for the non-linear increase in V_{OC} in Figure 5, upper left. Remarkably, at concentrations above 600×, the fill factor exhibits almost no dependence on temperature (Figure 5, upper right). The concentrator cell 1797-4-129-SCA-44 was designed to be operated at concentration ratios of approximately 500×, and the front-side metallisation was thus optimised for such irradiation levels. Consequently, the fill factor and efficiency decrease at higher concentrations as a result of series resistance losses. As a first approximation, the series resistance does not depend on temperature, which explains the reduced influence of the temperature on the fill factor at high concentrations shown in Figure 5 (upper right).

The temperature-dependent measurements shown in Figure 5 are not performed exactly at the same concentrations (except for the parameters determined at 1 sun using the multi-source simulator). To specify concentration-dependent temperature coefficients, a semi-logarithmic interpolation of the *I–V* parameters was applied and is indicated by the line graphs in Figure 5.

Temperature-dependent measurements as functions of concentration were performed using three multi-junction cells with different structures. The cell IDs, materials, band gaps at 25 °C and cell areas are summarised in Table I.

The temperature coefficients of the open circuit voltage V_{OC} and the efficiency η were determined at different concentration ratios. As a comparison of the results obtained from these three cells, Figure 6 shows the temperature coefficients of the open circuit voltages in absolute (mV/K, upper left) and relative forms (%/K, normalised by V_{OC} at 25 °C, upper right), the open circuit voltage at 25 °C (bottom left) and the relative temperature coefficient of the cell efficiency (relative %/K, normalised by the cell efficiency at 25 °C, bottom right).

All cells in Figure 6 exhibit the general behaviour expected from theory (compare Section 2): the open circuit voltage V_{OC} increases with concentration ratio and the temperature dependence of V_{OC}, and thus, efficiency also decreases with increasing concentration.

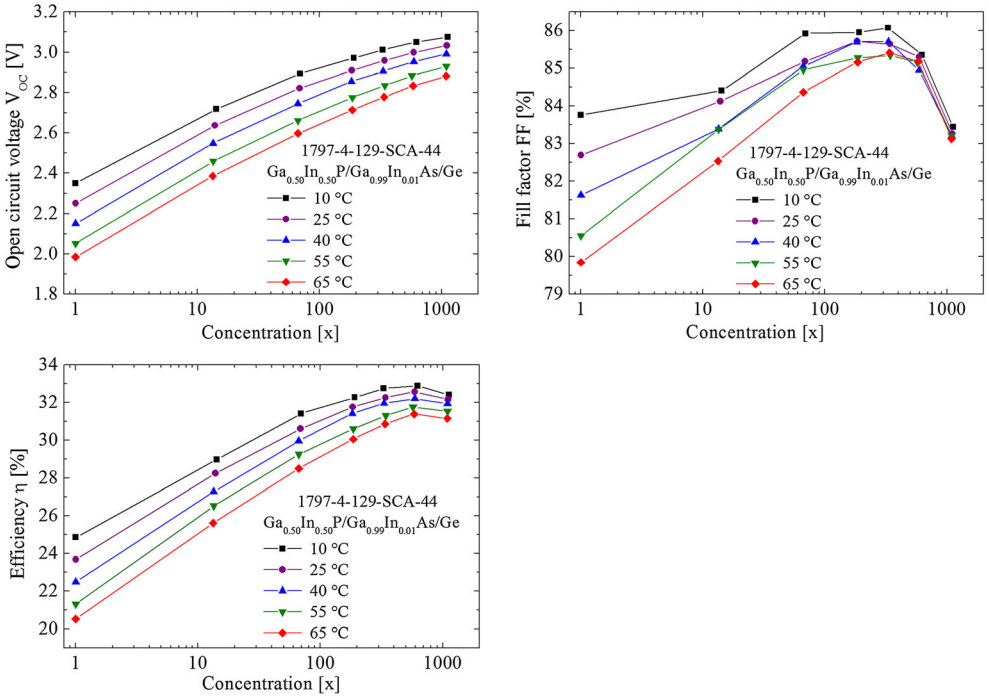

Figure 5. *I–V* parameters, open circuit voltage V_{OC} (upper left), fill factor *FF* (upper right) and efficiency η (bottom left) of the lattice-matched $Ga_{0.50}In_{0.50}P/Ga_{0.99}In_{0.01}As/Ge$ triple-junction cell 1797-4-129-SCA-44 versus concentration at different temperatures. The measurements under concentration were performed using the flash simulator, whereas those under 1-sun conditions were measured using the (steady state) multi-source sun simulator.

Table I. Cell IDs, material combinations, band gap energies at 25 °C and cell areas of the investigated multi-junction concentrator cells.

Cell ID	Material	E_g at 25 °C (eV)	Cell area (cm^2)
1797-4-129-SCA-44	$Ga_{0.50}In_{0.50}P/Ga_{0.99}In_{0.01}As/Ge$	1.9/1.4/0.7	0.0318
840-5-9	$Ga_{0.35}In_{0.65}P/Ga_{0.83}In_{0.17}As$	1.7/1.2	0.0351
1798-4-129-22-25	$Ga_{0.35}In_{0.65}P/Ga_{0.83}In_{0.17}As/Ge$	1.7/1.2/0.66	0.0318

The metamorphic triple-junction cell 1798-4-129-22-25 was only measured at concentrations up to 330×, as one of the tunnel diodes did not function properly at higher concentrations. Data of this cell have been included in the paper as they represent the first temperature-dependent data to be published on metamorphic $Ga_{0.35}In_{0.65}P/Ga_{0.83}In_{0.17}As/Ge$ triple-junction cells and as they show that temperature coefficients of such cells is in the same range as the ones of standard lattice-matched triple-junction cells.

To the first order, the differences in the values measured using 840-5-9 (squares in Figure 6, metamorphic $Ga_{0.35}In_{0.65}P/Ga_{0.83}In_{0.17}As$ dual-junction) and 1798-4-129-22-25 (triangles in Figure 6, metamorphic $Ga_{0.35}In_{0.65}P/Ga_{0.83}In_{0.17}As/Ge$ triple-junction cell) should be caused by the active germanium bottom cell of the triple-junction cell. Comparing the open circuit voltages (Figure 6, bottom left) of the two metamorphic cells, the gap between the V_{OC} values of the two cells increases with increasing concentrations, which can be explained by a stronger contribution from the germanium subcell when operating under concentration. The temperature coefficients of the two metamorphic cells exhibit a contrary behaviour. Because of the low band gap germanium subcell involved in the triple-junction cell, we expect that the triple-junction cell exhibits stronger temperature dependence. The temperature coefficient of the open circuit voltage (Figure 6, upper row) also exhibits a gap between the two metamorphic cells, and this gap again decreases with increasing concentrations. This trend corresponds to the expected reduction in the germanium subcell's sensitivity to temperature changes as the concentration increases. Interestingly, comparing the values of the relative temperature coefficient of V_{OC} (Figure 6, upper right), the lattice-matched triple-junction cell 1797-4-129-SCA-44 (circles in Figure 6) exhibits the weakest dependence on temperature, even though it includes a low band gap germanium subcell.

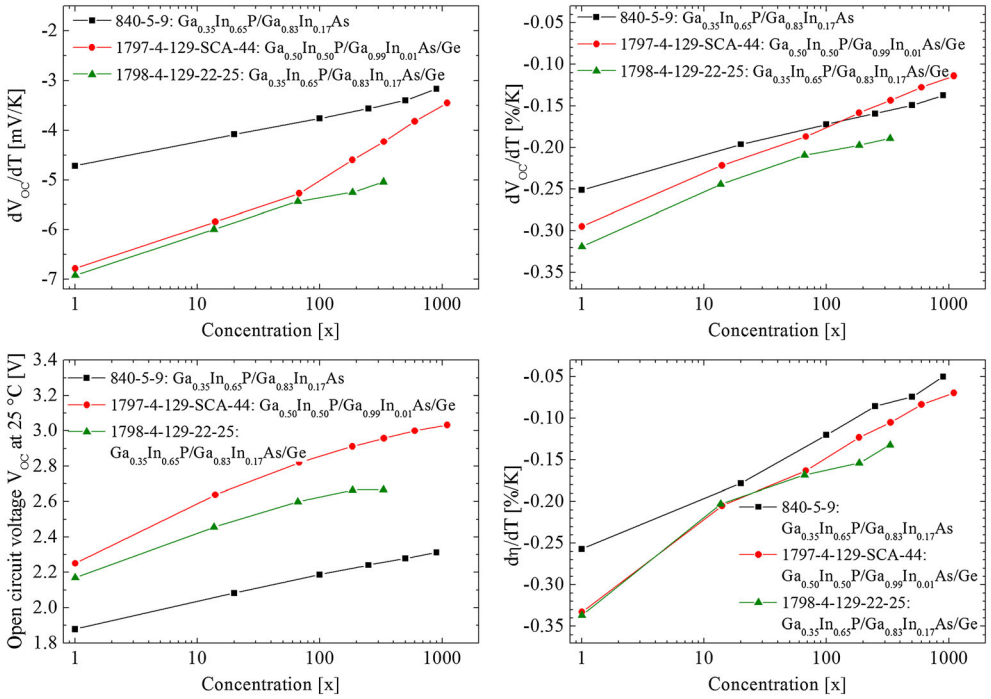

Figure 6. Summary of the temperature-dependent measurements performed on the three multi-junction cells described in Table I. Upper left: Temperature coefficient of the open circuit voltage V_{OC} in mV/K. Upper right: Temperature coefficient of V_{OC} presented in the relative units %/K, normalised by V_{OC} at 25 °C. Bottom left: Open circuit voltage V_{OC} at 25 °C versus concentration. Bottom right: Relative temperature coefficient of cell efficiency and thus the maximum power point in relative %/K, normalised by the cell efficiency at 25 °C.

The temperature coefficients and open circuit voltage V_{OC} at 25 °C shown in Figure 6 are summarised in Tables II–IV. The cell efficiency at 25 °C is also listed. No significant indication of non-linearity in the short circuit current versus irradiance was observed for the cell structures examined here. Therefore, the stated concentrations are based on the 1-sun I_{SC}, and the relative temperature coefficient of the short circuit current is valid for the entire concentration range.

4. SUMMARY AND CONCLUSION

The temperature dependence of the *I–V* parameters of multi-junction solar cells was investigated. The sensitivities of these temperature coefficients to changes in the spectrum were also analysed. Variations in the spectrum do not significantly change the temperature coefficients.

Temperature-dependent calibrations were performed on lattice-matched $Ga_{0.50}In_{0.50}P/Ga_{0.99}In_{0.01}As/Ge$ and on metamorphic $Ga_{0.35}In_{0.65}P/Ga_{0.83}In_{0.17}As$ dual-junction and $Ga_{0.35}In_{0.65}P/Ga_{0.83}In_{0.17}As/Ge$ triple-junction cells. A complete set of temperature coefficients versus concentration for the open circuit voltages and the efficiencies of these cells were determined. At concentrations between 300 and 500×, the temperature coefficients of the cell efficiencies (maximum power) of the three cells lie between −0.15 and −0.10%/K (relative %/K). The temperature coefficient of the maximum power under operation at 1-sun level is between −0.32 and −0.25%/K. Therefore, operation under concentration reduces temperature-related losses by a factor

Table II. Temperature coefficients of the open circuit voltage V_{OC} and the efficiency η and the values of V_{OC} and η at $T = 25$ °C versus concentration for the metamorphic $Ga_{0.35}In_{0.65}P/Ga_{0.83}In_{0.17}As$ dual-junction cell 840-5-9 (cell area 0.0351 cm^2).

C (x)	V_{OC} (25 °C) (mV)	η (25 °C) (%)	$TC_{abs}(V_{OC})$ (mV/K)	$TC_{rel}(V_{OC})$ (%/K)	$TC_{rel}(\eta)$ (rel. %/K)
1	1878	24.0	−4.71	−0.251	−0.257
20	2083	26.6	−4.08	−0.196	−0.178
100	2187	28.0	−3.76	−0.172	−0.120
250	2241	28.0	−3.56	−0.159	−0.085
500	2277	28.6	−3.39	−0.149	−0.074
900	2312	28.6	−3.17	−0.137	−0.050

The relative temperature coefficients for V_{OC} and η given in %/K were normalised by their respective values at 25 °C. The temperature coefficient of the short circuit current was determined to be 0.07%/K.

Table III. Temperature coefficients of the open circuit voltage V_{OC} and the efficiency η and the values of V_{OC} and η at $T = 25\,^{\circ}C$ versus concentration for the lattice-matched $Ga_{0.50}In_{050}P/Ga_{0.99}In_{0.01}As/Ge$ triple-junction cell 1797-4-129-SCA-44 (cell area 0.0318 cm^2).

C (x)	V_{OC} (25 °C) (mV)	η (25 °C) (%)	$TC_{abs}(V_{OC})$ (mV/K)	$TC_{rel}(V_{OC})$ (%/K)	$TC_{rel}(\eta)$ (rel. %/K)
1	2251	23.7	−6.79	−0.295	−0.333
14	2638	28.3	−5.84	−0.221	−0.205
68	2821	30.6	−5.27	−0.187	−0.163
185	2911	31.8	−4.60	−0.158	−0.123
335	2957	32.3	−4.23	−0.143	−0.105
600	2999	32.6	−3.82	−0.127	−0.083
1100	3032	32.2	−3.45	−0.114	−0.070

The relative temperature coefficients of V_{OC} and η given in %/K were normalised by their respective values at 25 °C. The temperature coefficient of the short circuit current was determined to be 0.06%/K.

Table IV. Temperature coefficients of the open circuit voltage V_{OC} and the efficiency η and the values of V_{OC} and η at $T = 25\,^{\circ}C$ versus concentration for the metamorphic $Ga_{0.35}In_{0.65}/Ga_{0.83}In_{0.17}As/Ge$ triple-junction cell 1798-4-129-22-25 (cell area 0.0318 cm^2).

C (x)	V_{OC} (25 °C) (mV)	η (25 °C) (%)	$TC_{abs}(V_{OC})$ (mV/K)	$TC_{rel}(V_{OC})$ (%/K)	$TC_{rel}(\eta)$ (rel.%/K)
1	2170	25.2	−6.92	−0.319	−0.337
13.6	2456	28.9	−5.99	−0.244	−0.203
66.2	2599	30.8	−5.43	−0.209	−0.168
185	2665	31.2	−5.25	−0.197	−0.154
331	2668	30.8	−5.04	−0.189	−0.132

The relative temperature coefficients of V_{OC} and η given in %/K were normalised by their respective values at 25 °C. The temperature coefficient of the short circuit current was determined to be 0.05%/K.

between 2 and 3. The main reason for this effect is the reduced temperature sensitivity of the open circuit voltage when operated under concentration (compare Section 2, theory and Figure 5). The temperature-related gain in the short circuit current makes the maximum power significantly less sensitive to temperature than the open circuit voltage (see Figure 6 and Tables II–IV).

REFERENCES

1. Crowley M. Why CPV? The CPV value proposition. SolarExpo, 2011.
2. Peharz G, Rodriguez JPF, Siefer G, Bett AW. A method for using CPV modules as temperature sensors and its application to rating procedures. *Solar Energy Materials and Solar Cells* 2011; **95**(10): 2734–2744.
3. Rubio F, Martinez M, Perea J, Sanchez D, Banda P. Comparison of the different CPV rating procedures: real measurements in ISFOC. Proceedings of the 34th IEEE Photovoltaic Specialists Conference, Philadelphia, 2009; 707–712.
4. Gueymard CA. Spectral circumsolar radiation contribution to CPV. Proceedings of the 6th International Conference on Concentrating Photovoltaic Systems, Freiburg, Germany, 2010; 316–319.
5. Kinsey GS, Stone K, Brown J, Garboushian V. Energy prediction of Amonix CPV solar power plants. *Progress in Photovoltaics: Research and Applications* 2011; **19**(7): 794–796.
6. Araki K. What is the most appropriate and practical index to represent spectrum sensitivity of CPV? Proceedings of the 6th International Conference on Concentrating Photovoltaic Systems, Freiburg, Germany, 2010; 205–208.
7. Sala G. Cooling of solar cells. In *Solar Cells and Optics for Photovoltaic Concentration*, Luque A (ed). IOP Publishing Ltd techno House: Bristol, England, 1989; 239–267.
8. Siefer G, Abbott P, Baur C, Schlegl T, Bett AW. Determination of the temperature coefficients of various III–V solar cells. Proceedings of the 20th European Photovoltaic Solar Energy Conference, Barcelona, Spain, 2005; 495–498.
9. Lee HS, Ekins Daukes NJ, Araki K, Kemmoku Y, Yamaguchi M. Field test and analysis: the behavior of 3-J concentrator cells under the control of cell temperature. Proceedings of the 31st IEEE Photovoltaic Specialists Conference, Orlando, Florida, USA, 2005; 754–757.
10. Aiken D, Stan M, Murray C, Sharps P, Hills J, Clevenger B. Temperature dependent spectral response measurements for III–V multi-junction solar cells. Proceedings

of the 29th IEEE Photovoltaic Specialists Conference, New Orleans, Louisiana, USA, 2002; 828–831.
11. Nishioka K, Takamoto T, Agui T, Kaneiwa M, Uraoka Y, Fuyuki T. Evaluation of temperature characteristics of high-efficiency InGaP/InGaAs/Ge triple-junction solar cells under concentration. *Solar Energy Materials and Solar Cells* 2005; **85**(3): 429–436.
12. Cotal HL, Sherif RA. Temperature dependence of the IV parameters from triple junction GaInP/InGaAs/Ge concentrator solar cells. Proceedings of the 4th World Conference on Photovoltaic Energy Conversion, Waikoloa, Hawaii, USA, 2006; 845–848.
13. Verlinden PJ, Lewandowski A, Bingham C, Kinsey GS, Sherif RA, Lasich JB. Performance and reliability of multijunction III–V modules for concentrator dish and central receiver applications. Proceedings of the 4th World Conference on Photovoltaic Energy Conversion, Waikoloa, Hawaii, USA, 2006; 592–597.
14. Siefer G, Bett AW. Calibration of III–V concentrator solar cells and modules. Proceedings of the 4th World Conference on Photovoltaic Energy Conversion, Waikoloa, Hawaii, USA, 2006; 745–748.
15. Kinsey GS, Hebert P, Barbour KE, Krut DD, Cotal HL, Sherif RA. Concentrator multijunction solar cell characteristics under variable intensity and temperature. *Progress in Photovoltaics: Research and Applications* 2008; **16**: 503–508.
16. Kinsey GS, Edmondson KM. Spectral response and energy output of concentrator multijunction solar cells. *Progress in Photovoltaics: Research and Applications* 2009; **17**(5): 279–288.
17. Chiu P, Wojtczuk S, Harris C, Pulver D. Temperature dependence of InGaP/GaAs/InGaAs concentrators using bifacial epigrowth. Proceedings of the 37th IEEE Photovoltaic Specialists Conference, Seattle, Washington, USA, 2011.
18. Steiner MA, Geisz JF, Friedman DJ, Olavarria WJ, Duda A, Moriarty T. Temperature-dependant measurements of an inverted metamorphic multijunction (IMM) solar cell. Proceedings of the 37th IEEE Photovoltaic Specialists Conference, Seattle, Washington, USA, 2011.
19. Landis GA, Belgiovane DJ, Scheiman DA. Temperature coefficient of multijunction space solar cells as a function of concentration. Proceedings of the 37th IEEE Photovoltaic Specialists Conference, Seattle, Washington, USA, 2011; 1–6.
20. Kurtz SR, Faine P, Olson JM. Modeling of two-junction, series-connected tandem solar cells using top-cell thickness as an adjustable parameter. *Journal of Applied Physics* 1990; **68**(4): 1890–1895.
21. Faine P, Kurtz SR, Riordan C, Olson JM. The influence of spectral solar irradiance variations on the performance of selected single-junction and multijunction solar cells. *Solar Cells* 1991; **31**(3): 259–278.
22. Adelhelm R, Bücher K. Performance and parameter analysis of tandem solar cells using measurements at multiple spectral conditions. *Solar Energy Materials and Solar Cells* 1998; **50**(1–4): 185–195.
23. Meusel M, Adelhelm R, Dimroth F, Bett AW, Warta W. Spectral mismatch correction and spectrometric characterization of monolithic III–V multi-junction solar cells. *Progress in Photovoltaics: Research and Applications* 2002; **10**(4): 243–255.
24. Wuerfel P. *Physics of Solar Cells—from Principles to New Concepts*. Wiley-VCH Verlag: Weinheim, Germany, 2005.
25. Fan JCC. Theoretical temperature dependence of solar cell parameters. *Solar Cells* 1986; **17**: 309–315.
26. Friedman DJ. Modelling of tandem cell temperature coefficients. Proceedings of the 25th IEEE Photovoltaic Specialists Conference, Washington DC, USA, 1996; 89–92.
27. Varshni YP. Temperature dependence of the energy gap in semiconductors. *Physica* 1967; **34**(1): 149–154.
28. Thurmond CD. The standard thermodynamic functions for the formation of electrons and holes in Ge, Si, GaAs, and GaP. *Journal of the Electrochemical Society* 1975; **122**(8): 1133–1141.
29. DeMoulin PD, Tobin SP, Lundstrom MS, Carpenter MS, Melloch MR. Influence of perimeter recombination on high-efficiency GaAs p/n heteroface solar cells. *IEEE Electron Device Letters* 1988; **9**(8): 368–370.
30. Díaz V, Algora C. Influence of perimeter recombination in the design of very high concentrator GaAs solar cells. Proceedings of the16th European Photovoltaic Solar Energy Conference, Glasgow, UK, 2000; 1034–1037.
31. Stellwag TB, Dodd PE, Carpenter MS, Lundstrom MS, Pierret RF, Melloch MR, Yablonovitch E, Gmitter TJ. Effects of perimeter recombination on GaAs based solar cells. Proceedings of the 21st IEEE Photovoltaic Specialists Conference, Kissimmee, Florida, USA, 1990; 442–447.
32. Seaman CH. Calibration of solar cells by the reference cell method—the spectral mismatch problem. *Solar Energy* 1982; **29**(4): 291–298.
33. Adelhelm R, Bartlau J, Bücher K. Temperature coefficients of tandem solar cells under appropriate spectra. Proceedings of the 14th European Photovoltaic Solar Energy Conference, Barcelona, Spain, 1997; 1736–1739.
34. Burdick J, Glatfelter T. Spectral response and *I–V* measurements of tandem amorphous-silicon alloy solar cells. *Solar Cells* 1986; **18**(3–4): 301–314.